Evaluating Observation Influence on Regional Water Budgets in Reanalyses

MICHAEL G. BOSILOVICH

Global Modeling and Assimilation Office, NASA Goddard Space Flight Center, Greenbelt, Maryland

JIUN-DAR CHERN

Earth System Science Interdisciplinary Center, University of Maryland, College Park, College Park, Maryland

DAVID MOCKO

SAIC, and Global Modeling and Assimilation Office, Greenbelt, Maryland

FRANKLIN R. ROBERTSON

NASA Marshall Space Flight Center, Huntsville, Alabama

ARLINDO M. DA SILVA

Global Modeling and Assimilation Office, NASA Goddard Space Flight Center, Greenbelt, Maryland

(Manuscript received 4 September 2014, in final form 30 January 2015)

ABSTRACT

The assimilation of observations in reanalyses incurs the potential for the physical terms of budgets to be balanced by a term relating the fit of the observations relative to a forecast first guess analysis. This may indicate a limitation in the physical processes of the background model or perhaps assimilating data from an inconsistent observing system. In the MERRA reanalysis, an area of long-term moisture flux divergence over land has been identified over the central United States. Here, the water vapor budget is evaluated in this region, taking advantage of two unique features of the MERRA diagnostic output: 1) a closed water budget that includes the analysis increment and 2) a gridded diagnostic output dataset of the assimilated observations and their innovations (e.g., forecast departures).

In the central United States, an anomaly occurs where the analysis adds water to the region, while precipitation decreases and moisture flux divergence increases. This is related more to a change in the observing system than to a deficiency in the model physical processes. MERRA's Gridded Innovations and Observations (GIO) data narrow the observations that influence this feature to the ATOVS and *Aqua* satellites during the 0600 and 1800 UTC analysis cycles, when radiosonde information is not prevalent. Observing system experiments further narrow the instruments that affect the anomalous feature to AMSU-A (mainly window channels) and Atmospheric Infrared Sounder (AIRS). This effort also shows the complexities of the observing system and the reactions of the regional water budgets in reanalyses to the assimilated observations.

1. Introduction

Critical evaluation of the Modern-Era Retrospective Analysis for Research and Applications (MERRA; see appendix for acronym definitions) global water and energy budgets has documented significant improvements over previous generations of reanalysis in the annual-mean spatial patterns and amounts of precipitation in NASA's latest reanalysis such that skill relative to GPCP/CMAP uncertainties is equivalent to that of the Interim ECMWF Re-Analysis (ECMWF-Interim; Bosilovich et al. 2011). There are, nevertheless, areas where improvements can be made in the

Corresponding author address: Michael G. Bosilovich, Global Modeling and Assimilation Office, Code 610.1, NASA Goddard Space Flight Center, Greenbelt, MD 20771.
E-mail: michael.bosilovich@nasa.gov

DOI: 10.1175/JCLI-D-14-00623.1

hydrologic and energy cycles of this reanalysis (and other contemporary reanalyses as well). For example, regional water cycles exhibit biases and generally depend on the density and variability of observations available for assimilation. The extent of these uncertainties can be deduced from the magnitude and behavior of the nonphysical increment terms of state variable conservation equations (e.g., u for zonal wind, v for meridional wind, T for air temperature, q for water vapor specific humidity). The analysis increments provide a wealth of information as to the biases in model physics as well as the utility and veracity of the observations being assimilated. Bosilovich et al. (2011) and Robertson et al. (2011) show that (i) systematic regional biases in vertically integrated moisture and heat budgets exist as manifestations of physics parameterization weaknesses and (ii) these model biases interact with an evolving satellite observing system to cause spurious changes in fluxes produced by the assimilation.

For example, Trenberth et al. (2011) found that, in MERRA and ERA-Interim (Dee et al. 2011), atmospheric moisture divergence [which theoretically relates globally to evaporation (E) minus precipitation (P)] shows positive values over a substantial portion of the United States for a long time average. The land/atmosphere budget of water does not allow for continental-scale $E > P$ over long time periods, so this result, sometimes called an imbalance, is not physical. In a data assimilation system, this nonphysical result is generated while numerically correcting the mass in the direction of observations over long periods of time. MERRA provides the analysis tendencies that can be used to diagnose closed budgets, but these tendencies represent the effect of the entire observing system at the analysis time. To better understand the source of these tendencies, it should be useful to evaluate the individual observing systems for 1) data availability and 2) which observing system is most closely related to the eventual analysis. While the impact of observational systems on analyses has been studied in respect to forecast error reduction (e.g., Gelaro and Zhu 2009), here we are focusing on the regional water vapor balance.

Figures 1a,b show the moisture flux divergence (MFD) from MERRA and ERA-Interim (Dee et al. 2011) for the period 2001–12. The positive MFD area over the central United States is a feature noted by Trenberth et al. (2011), who point out that there is no accounting of irrigation in the MERRA or ERA-Interim land parameterization (although ERA-Interim surface meteorology analysis does adjust soil moisture). In the region where this anomalous divergence occurs, irrigation can make a contribution to surface evaporation (Ozdogan and Gutman 2008; Ozdogan et al. 2010). In evaluations of the central United States water cycle, lack of irrigation in the model may contribute to water vapor biases that the analysis should strive to overcome. For example, large bodies of water (Great Salt Lake and Great Lakes) register as long-term divergent regions in Fig. 1. However, it is not clear that the radiosonde network has enough data to close a regional water budget and then reconcile irrigation contributions to MFD (Yarosh et al. 1999; Kanamaru and Salvucci 2003). This comparison opens up numerous questions and is far from clear about the underlying causes of the imbalance. Is it seasonally or diurnally varying? This is a short period in the MERRA record: does it hold for the 30 yr? Are the imbalances in MERRA and ERA-Interim occurring for similar reasons? Since this is an unphysical result, it is likely related to the observational analysis. Which component(s) of the observing system contributes to this inconsistency? The objective of this study is to use some unique MERRA diagnostic output to better understand this feature and how it came to be present in the water cycle data.

2. Data

a. MERRA

MERRA is the first reanalysis produced at NASA since the early 1990s [more completely described by Rienecker et al. (2011)]. The objective of the project is to provide reanalysis data for the science community but also to make some improvement of the water cycle beyond existing reanalyses. In November 2007, the GMAO completed a validation of the GEOS5 data assimilation system for MERRA, finding that the global total column water and precipitation exhibited spatial statistics better than existing (at that time) reanalyses, but spurious time variations of the mean water cycle were related to changes of the observational record. This is confirmed in the resulting MERRA data (Bosilovich et al. 2011), and at large scales MERRA is providing water cycle data better than the previous generation of reanalyses and as good as or better than the other most recent reanalyses. Of course, the water cycle still requires development in many areas.

The MERRA data assimilation system (GEOS5) also includes some unique attributes that affect the water cycle evaluation. The system uses a three-dimensional variational assimilation scheme, but the model states are updated incrementally [incremental analysis updates (IAU), as described by Bloom et al. (1996)]. While the IAU does significantly reduce shock of the analysis on

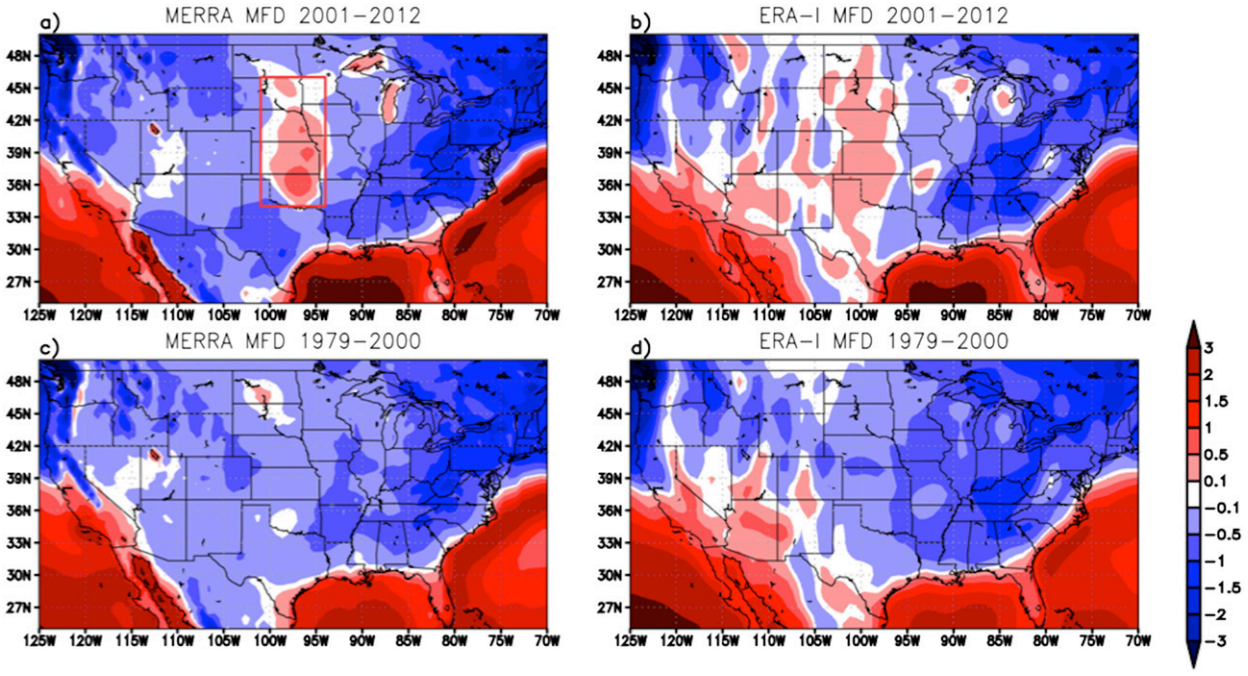

FIG. 1. Mean vertically integrated moisture flux divergence (mm day^{-1}) from (left) MERRA and (right) ERA-Interim (Dee et al. 2011) reanalyses for (top) 2001–12 and (bottom) 1979–2000. The red box in (a) indicates the central U.S. region (34°–46°N, 101°–94°W) that has positive moisture flux divergence for 2001–12.

precipitation, it also provides a tendency term in the moisture budget (as well as heat and momentum) for the observational analysis,

$$\frac{\partial w}{\partial t} = -\nabla \cdot \overline{(\mathbf{V}w)} + (E - P) + \left[\frac{\partial w}{\partial t}\right]_{\mathrm{ANA}} + \left[\frac{\partial w}{\partial t}\right]_{\mathrm{CHM}} + \left[\frac{\partial w}{\partial t}\right]_{\mathrm{FIL}}. \quad (1)$$

The terms of the GEOS5/MERRA total vertically integrated atmospheric water (w, which includes vapor, liquid and ice phases) budget are total water tendency, moisture flux convergence (i.e., −MFD), surface evaporation (E), liquid and solid precipitation (P), and the analysis tendency (ANA). A negative fill correction (FIL) is included in the model to prevent spurious occurrences of negative water vapor (in the region evaluated here, and this version of the model, this term is present but zero value). A chemistry conversion term (CHM) is included, but in MERRA this relates primarily to stratospheric water vapor and the vertically integrated tendency is typically less than 0.04% of precipitation or evaporation for the global average. ANA and FIL represent nonphysical changes to the reanalysis water vapor budget, while the other terms are related to physical processes. The chemistry and fill terms are small or zero in this study and will not be evaluated. The vertical integration is performed during the cycling of the data on model native vertical coordinate. The analysis tendency term (derived from IAU method discussed above and referred to here as ANA) originates with the observational analysis and provides a diagnostic value of the mean departure from observations (as an aggregate of all assimilated observations). In some studies that consider this influence on the water budget, the term was solved as a residual (e.g., Roads et al. 2002; Yokoi 2015) from the vertically integrated water budget, but with MERRA the full water budget is produced, including vertically integrated quantities from the model's vertical grid. A key point here is that the ANA term is not just a measure of imbalance but has spatially (3D) and temporally varying structure related to the comparison of the background forecast model with the available observations.

b. GIO

The observations and forecast departures resulting from the data assimilation process are typically stored in observation-space formatted files, in that they have coordinates in space and time to their exact location, unique to each observation record. This level of spatiotemporal precision for data assimilation is required to make the best use of the observations and to diagnose the eventual analysis. However, the data formats can be

more diverse than typical reanalysis output and may vary depending on the instrument. Likewise, missing records can complicate evaluation. To more easily compare multiple instruments and observing systems, and simplify the data access, we have developed the Gridded Innovations and Observations (GIO) dataset. Assimilated data are binned to the native MERRA analysis grid in space and time (⅔° longitude by ½° latitude, 42 pressure levels, and 6-hourly synoptic times), for each observing platform and observations type, as well as instrument and channel. The data files include the observation, forecast departure [observation minus forecast (OmF)], and analysis departure [observation minus analysis (OmA)]. It is worthwhile to note that the variational bias correction (Dee and Uppala 2009) term is included with the OmF values. If multiple observations from the same observing system are binned in the same grid space, they are averaged and the GIO files also include the data count and standard deviation in each bin.

While evaluating this particular gridded data, one must consider that the spatial and temporal coverage by each sensor type is not homogeneous and all grid points may not have the same number of binned observations. Instead, we must make use of both the observation value and the number of observations in a grid box. For example, monthly-mean temperature (T) can be determined from 6-hourly binned temperature (T') by

$$T = \sum_{t=1}^{M} T'(t) \times n(t) \Big/ \sum_{t=1}^{M} n(t), \qquad (2)$$

where M is the number of 6-hourly analyses cycles in a month and n is the number of observations that were used to create the binned temperature. Likewise, area averages must consider the total number of observations over the area. If the data were in observations space, then this is essentially how the average would be computed. The important point is that the gridded data include the number of observations that create the binned average, and considering the number of observations is important to appropriately average boxes with many observations and those with few. The advantage of gridded data is that the uniform file formats can be more easily evaluated in standard software and file sizes are much smaller. Caution must still be exercised in that small numbers of observations or asymmetric distributions of observations may significantly affect time and space averaging.

Here, we refer to physical observations or retrieved satellite observations that are assimilated as ''conventional'' observations, distinguishing those from remotely sensed radiances (Rienecker et al. 2011). In terms of data volume, the conventional observations are smaller than the radiance observations, and so are merged together in a single collection of different variables, whereas each assimilated channel's radiance observations are collected with its respective instrument (e.g., MSU, SSU, AMSU, HIRS, and SSM/I) and satellite. Conventional observations with a vertical dimension (such as radiosondes) are likewise binned to MERRA's vertical grid (42 pressure levels). Having the assimilated observations in a gridded format allows simplified inspection of the data availability in space and time and across all the varying systems, platforms, instruments, orbits, and channels. In general, gridding does provide a cost savings for the radiance data, as the spatial resolution can be very high, even if much of the globe is not observed during an assimilation cycle for a given instrument. Data distribution in space and time, relative to the region of interest, will be discussed in sections 3c and 3d.

c. *MERRA-Land*

Recognizing that the atmospheric forcing above the land surface can be biased because of atmospheric model biases, Reichle et al. (2011) developed MERRA-Land. This is a reprocessing of the land model parameterization (only), using bias corrected precipitation in place of the model-generated precipitation that provides the water source for land in MERRA. Other forcings are derived from MERRA. The bias correction ensures that, at long periods, the MERRA-Land precipitation reflects observed values. In this way, we can also assess MERRA precipitation bias and any consequence that may have in the budget analysis, whereas MERRA-Land provides a comparison for P, E, and $E - P$ that we may expect to have some higher quality than MERRA itself.

3. Water budget evaluation

a. *Vertically integrated water budget climatology*

The main purpose of this paper is to investigate the long-term MFD pointed out by Trenberth et al. (2011) and shown in Figs. 1a,b. This feature is not persistent throughout the period of the satellite-era reanalyses (Figs. 1c,d). Considering the area average for the central United States (region demarcated by the red box in Fig. 1a), the transition into excessive MFD is a jump in the regions time series (Fig. 2). Interestingly, MERRA's transition occurs around 2000, while ERA-Interim (Dee et al. 2011) experiences a jump in 1994. ERA-Interim uses the same conventional observations as ERA-40 through 2001. ERA-40 transitions from historical data sources to the ECMWF operational feed in 1994,

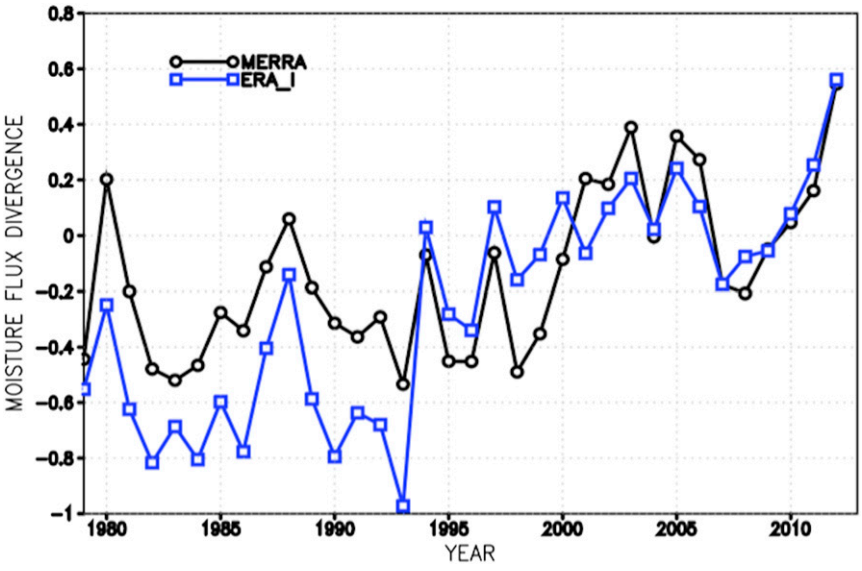

FIG. 2. Time series of annual-mean vertically integrated moisture flux divergence (mm day^{-1}) over the central United States (red box in Fig. 1a) from the MERRA and ERA-Interim reanalyses.

resulting in a change in the number of assimilated observations (Uppala et al. 2005). This change in conventional observation data streams could influence the water cycle analysis.

The inconsistency in timing between MERRA and ERA-Interim suggests that the underlying causes in each system are likely different. The subsequent analysis focuses on MERRA because of this disparity in the time series and occurrences of the change but also because MERRA includes more output diagnostics readily available than ERA-Interim. This temporal variation was not presented by Trenberth et al. (2011), but we will use the disparity between the years before and after 2001 to identify the impact and causes of the shift. In the subsequent evaluations, we considered that the shift may be related to a physical process (e.g., sea surface temperature through teleconnections or lack of irrigation at the land surface) or assimilated data (type, quantity, or quality), but ultimately it becomes clear that observing system changes are a primary consideration.

Over long periods, terms for total tendency and corrections (as discussed earlier) can be neglected in Eq. (1). The remaining terms of the vertically integrated water balance are provided in Fig. 3. The first noticeable comparison is that the analysis increment (ANA) pattern over land matches closely the MFD pattern, even in negative (moisture converging) regions. The interactions with the surface are apparent as well, for example, the Great Lakes appear as a source of atmospheric water for divergence in $E - P$. However, the sudden shift to positive analysis increments in 2000 seems to rule out a missing surface evaporative source causing the central U.S. positive MFD. There is not an obvious correlation between the central U.S. E, P, or $E - P$ and ANA, which suggests the water vapor being added through the analysis is contributing to MFD. However, this is not to say that an appropriate accounting of irrigation in the reanalysis is unimportant.

For most of the 34-yr period, MERRA precipitation is lower than MERRA-Land in the central United States (Fig. 4a; keeping in mind that MERRA-Land precipitation is bias corrected by CPCU rainfall observation data). The evaporation in both datasets is strongly constrained by the precipitation, and MERRA central U.S. evaporation then should be underestimated. If we consider that, in a physical sense, $E - P$ should be long-term moisture flux divergence, both MERRA and MERRA-Land $E - P$ have a similar interannual variability (Fig. 4b). However, MERRA periods of negative $E - P$ (convergence) seem to be somewhat weaker amplitude compared to those in MERRA-Land. It is also clear that MERRA $E - P$ shows little resemblance to MFD interannual variability. The MFD interannual variability tracks very closely with the analysis increment, especially the strong shift around 2000 that leads to the divergent area in Figs. 1 and 3. To emphasize this, Table 1 shows correlations of the annual-mean time series of the central U.S. MERRA water

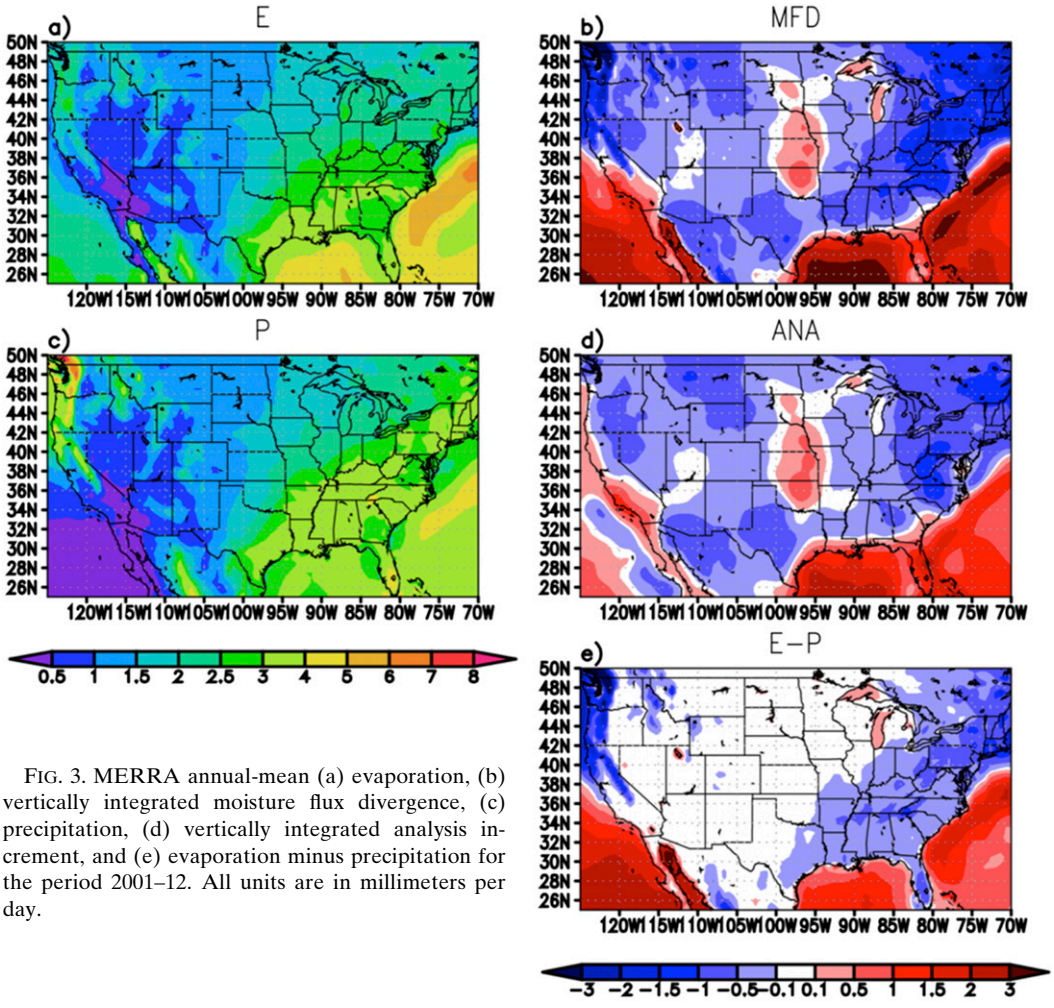

FIG. 3. MERRA annual-mean (a) evaporation, (b) vertically integrated moisture flux divergence, (c) precipitation, (d) vertically integrated analysis increment, and (e) evaporation minus precipitation for the period 2001–12. All units are in millimeters per day.

budget terms (which are shown in Fig. 4). The strongest interannual relationships seem to be between ANA and MFD, and also between P and E. Since there is no data assimilation in the land surface, at long time scales E follows P, leading to a high correlation. Given that precipitation exhibits a mean low bias against observations, it could be argued that positive water vapor increments should increase the precipitation, rather than the divergence. The subsequent evaluation of the water budget will better explain the reanalysis data in this region.

Figure 5 compares the mean annual cycle of the vertically integrated water budget before and after the shift in the early 2000s. Despite substantial reductions in both E and P in more recent times, $E - P$ remains stable across the shift, again, as E is limited by P in the land model. However, MFD and ANA increase substantially across the shift mainly during the warm and wet seasons (relative to atmospheric temperature and humidity) from spring through early fall, with differences peaking in July and August. The ANA increments are positive from June to September, adding water to the column, especially after the shift. The $E - P$ mean annual cycle peaks in early summer, 1–2 months earlier than that of MFD, and is substantially weaker than the latter. The additional water from ANA is contributing to the increase of MFD, but it is not intuitive as yet, why the precipitation should decrease. The total water tendencies are small and do not change across the shift (not shown).

The mean diurnal cycle (for all seasons) is characterized in Fig. 6, including the comparison around the 2001 shift. One feature worth explaining first is the ANA diurnal cycle. MERRA produces four analyses at each of 0000, 0600, 1200, and 1800 UTC.[1] This defines the analysis increment, which for an analysis time is

[1] Note that ERA-Interim 4D variational assimilation is cycled every 12 h which reduces sensitivity to differences between 0000/1200 UTC and 0600/1800 UTC times.

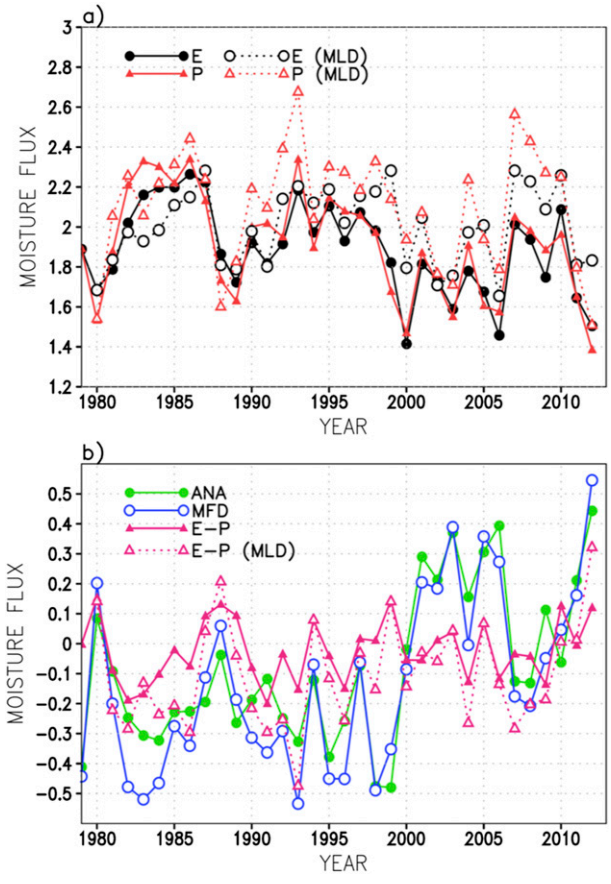

FIG. 4. Time series of annual-mean vertically integrated moisture budget (mm day^{-1}) over the central United States from MERRA and MERRA-Land (MLD).

determined over the previous 6 h, is carried backward in time and is used to determine the analysis tendency, termed ANA here, for the water budget in a separate model integration [this is called the assimilation cycle; more details are explained by Rienecker et al. (2011)]. The ANA tendency is fixed for the 6-h assimilation cycle and when plotted in an hourly diurnal cycle appears constant for each 6-h period and steps to the next time period. Before 2001, the mean 0000 and 1200 UTC analysis increments are small, close to zero. After 2001, the 1200 UTC analysis increments add water to the column, but 0000 UTC increments remove water from the column. This systematic diurnal cycle of ANA after 2001 can be problematic, repeatedly adding water then removing it will be detrimental to the regional water cycle. Before 2001, 1800 and 0600 UTC each act to remove water from the system at a relatively low rate. The diurnal cycle of the ANA vertical profiles will be discussed further in the next section.

TABLE 1. Time correlation coefficients of annual-mean water budget terms over the central United States from 1979 to 2012.

	P	E	$E-P$	MFD
E	0.92	1.00		
$E-P$	−0.54	−0.18	1.00	
MFD	−0.79	−0.69	0.51	1.00
ANA	−0.66	−0.71	0.15	0.93

The reduction in precipitation after 2001 is spread across the diurnal cycle. Of course, evaporation is small at night, so the reductions in water stored in the surface mostly affect the daytime maximum of evaporation. There is a general increase of divergence across the diurnal cycle, with increased daytime divergence and less nighttime convergence after 2001. A substantial portion of the increased divergence occurs from 0600 through 1500 UTC when the ANA term is adding water to the system. However, at any given hour of the mean diurnal cycle, the total tendency may also be nonzero. The ANA term affects first the water content as evidenced by the total tendency and then MFD catches up after some time. During the drier daytime (relative to surface evaporation and smaller total positive change), the analysis increment is not adding water, but divergence is removing it from the region. If the analysis were working to compensate for low evaporation at the surface, the 1800 UTC increment would be the most direct way to make that adjustment. With few radiosondes in the 1800 UTC analysis, the increments rely primarily on remotely sensed observations. Satellite data will be considered in section 3d.

b. *Three-dimensional water vapor budget*

While it is often convenient to study the vertically integrated water vapor budget, physical, dynamical, and assimilation processes are occurring in three dimensions and so the vertical distribution of the tendencies can be important in understanding the budget. Figure 7 compares the vertical section of main terms of Eq. (1) with annual area averages for the central U.S. region. Here, "MST" represents the moist precipitation processes (condensation and rain evaporation) while "TRB" represents the turbulent tendencies (which vertically integrates to surface evaporation). Note that MST represents the atmospheric water vapor tendency due to precipitation (and rain evaporation), so that condensation is negative. The full field and anomalies from the mean are shown to demonstrate the interannual variability of the terms. Some of the largest changes in the precipitation tendency (MST; Figs. 7e,f) occur within the boundary layer (between the surface and 800 hPa), where condensation is being substantially reduced. The

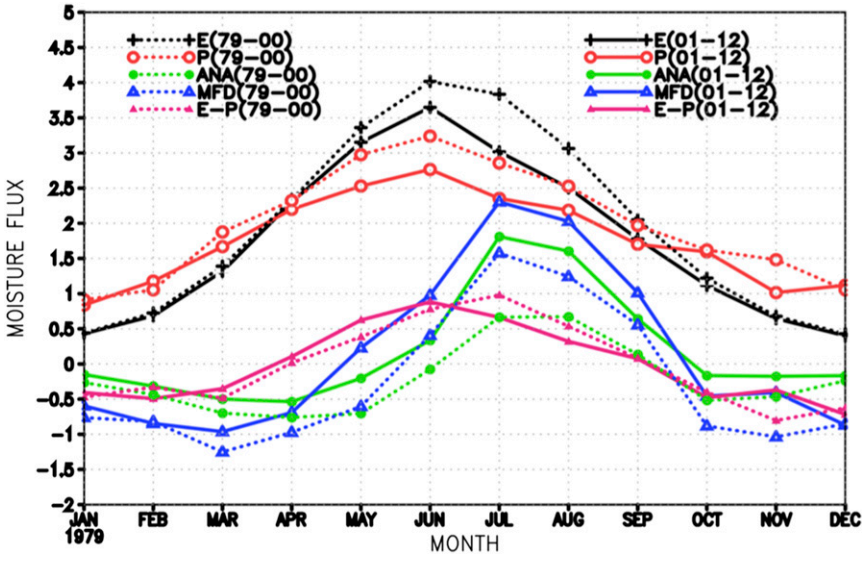

FIG. 5. Annual cycle of vertically integrated moisture budget (mm day^{-1}) over the central United States for the periods 1979–2000 (dotted lines) and 2001–12 (solid lines).

analysis increment is adding some water back in the PBL (Figs. 7c,d). After 2001, the analysis is adding more water in the middle troposphere (between 800 and 500 hPa), where it contributes to increasing divergence (Fig. 7b). The turbulent tendency (Fig. 7h) reflects the reduction in surface evaporation. Since the only source of water for land evaporation is precipitation, the changes in evaporation are following that of the precipitation. Figure 8 shows a comparison of the water budget tendency profiles before and after 2001. The

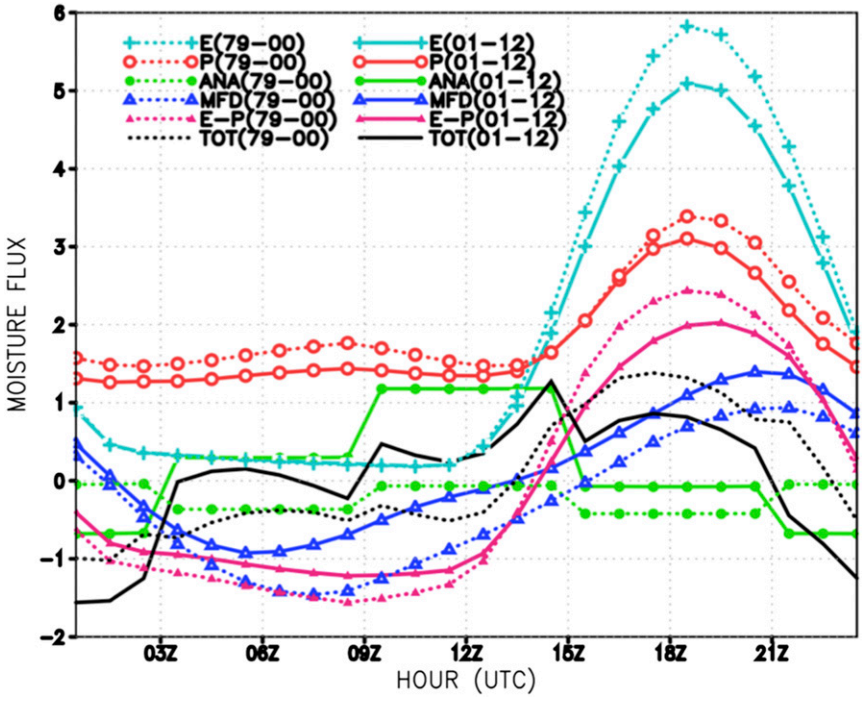

FIG. 6. Diurnal cycle of vertically integrated moisture budget (mm day^{-1}) over the central United States for the periods 1979–2000 (dot lines) and 2001–12 (solid lines). Local time can be approximated by UTC minus 6 h.

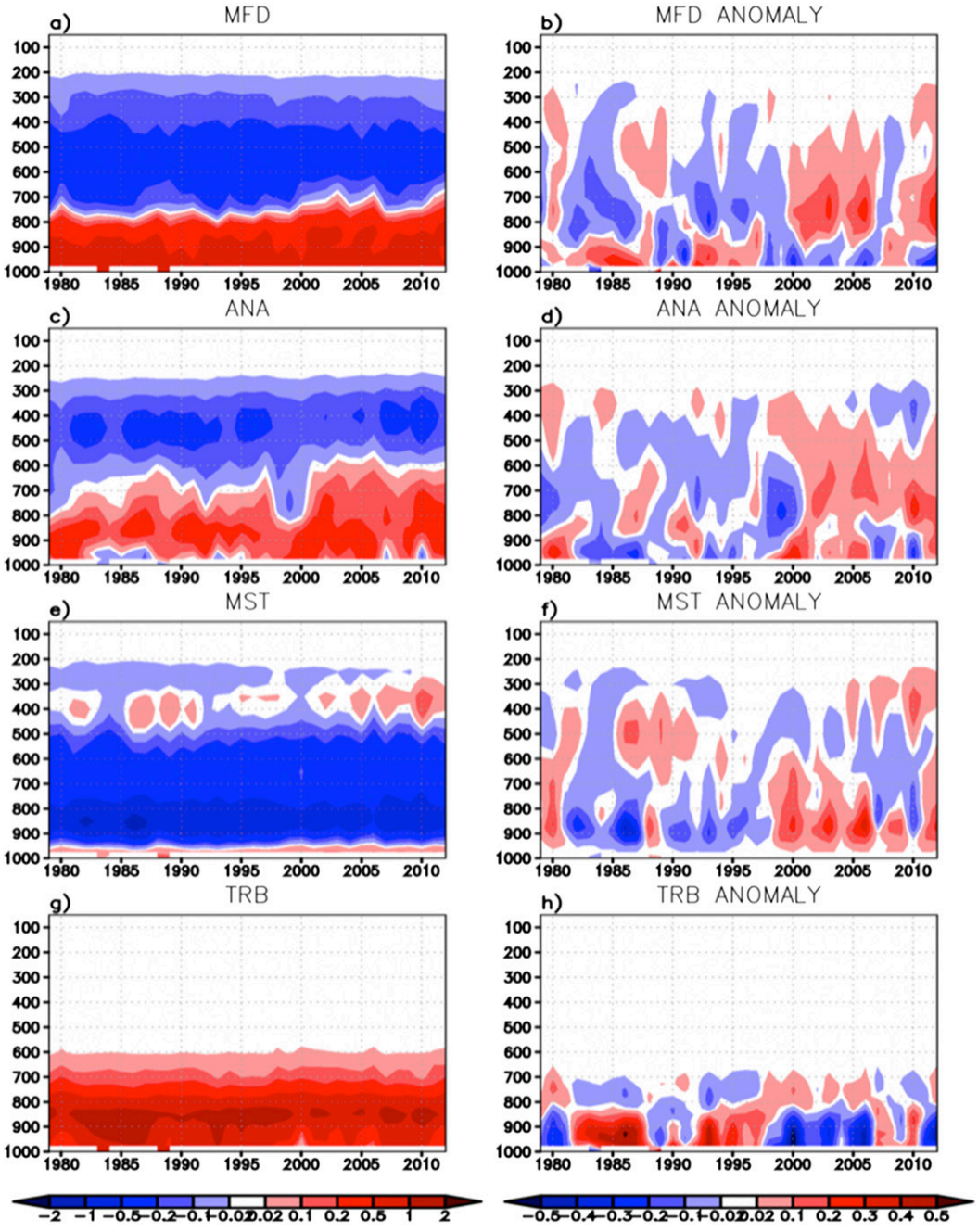

FIG. 7. Time–height cross section of (left) annual-mean water vapor tendency terms over the central United States and (right) their anomalies from the 1979–2012 climate mean. All units are in g kg^{-1} day^{-1}. Here, MST represents the precipitation processes (including all phases of condensation and rain evaporation) and TRB represents turbulence tendencies (vertically integrates to surface evaporation).

peak reduction of water in the column due to precipitation processes (MST) has a maximum at the top of the boundary layer (Figs. 7e,f and 8b). Turbulent mixing provides a large source of water for precipitation in the upper portion of the boundary layer and is significantly reduced after 2001 (Figs. 7g,h and 8b). While the analysis increment is positive (adding water due to the observational analysis), the change after 2001 is primarily above 800 hPa (Figs. 7c,d and 8a). The question remains, if the analysis is adding water into the lower atmosphere and boundary layer, then why does precipitation decrease?

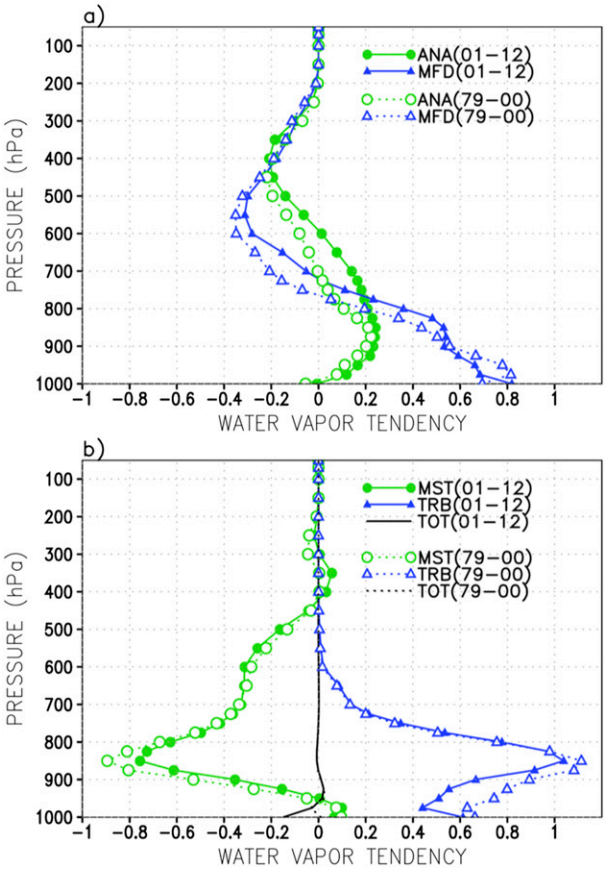

FIG. 8. Vertical profiles of water vapor tendency terms ($g\,kg^{-1}\,day^{-1}$) over the central United States for the periods 1979–2000 (dotted lines) and 2001–12 (solid lines).

In separating the analysis increment into time series for each of the diurnal analysis times (Fig. 9), we find distinct interannual variations for each analysis time. However, the analyses with most radiosonde observations (0000 and 1200 UTC) are very different from those with few radiosondes (0600 and 1800 UTC). For example, at 0600 UTC analysis tendencies for water vapor were quite small (and uniformly negative throughout the column) until early 2001, when they become abruptly large positive between 800 and 500 hPa. This shift is toward strongly positive increments at 700 hPa, mostly above the boundary layer. A similar shift occurs in the 1800 UTC analysis time, though it becomes strongest in early 2003. To objectively identify a time of this transition, we use the changepoint test developed by Lund and Reeves (2002) on the 700-hPa water vapor increments. The result indicates a statistically significant changepoint in April 2001 at 0600 and 1800 UTC (though the 1800 UTC maximum in the changepoint test is found in February 2003). Conversely, 0000 and 1200 UTC analysis increments do not yield any statistically significant changepoints. The presence of radiosondes may provide a stabilizing factor, or at least any changes in the radiosonde observing system are not enough to make a significant shift in the time series. For the whole reanalysis period, the 1200 UTC (early morning) analysis is adding water into the lowest layers of the troposphere. The analysis increment at 1800 UTC is removing water from within the boundary layer during the daytime (Fig. 6) when MERRA produces most precipitation in this region. Figure 10 compares the mean profiles of ANA and MFD before and after 2001. The 0600 and 1800 UTC change in ANA is pronounced. What were once small increments have increased magnitude substantially, and the 0600 and 1800 UTC MFD changes follow the ANA vertical distribution. It seems likely then that the ANA reduction in daytime (1800 UTC) boundary layer moisture is slowing the production of precipitation, which in turn is the limit of land evaporation. This is contrary to the 1200 UTC (morning) analysis increments. Before 2001, the 1200 UTC increments were tending to add moisture to the lowest layers; after 2001, this tendency doubled. The 0000 and 1200 UTC analyses include the substantial radiosonde observation coverage, which in turn also constrain the analysis of satellite radiances, through variational bias correction (Dee and Uppala 2009). To evaluate this further, information on the observations is needed.

4. Observing system evaluation

a. *Observing system characteristics*

In the discussion to this point, the ANA term of the water vapor budget includes the combined information from all the assimilated observing systems, when the spatiotemporal distribution of all the different observing systems is quite complex to characterize. Figure 11 shows the spatial and temporal data count of radiosonde derived specific humidity in MERRA at 0000 and 1200 UTC [ARM Southern Great Plains (SGP) in Oklahoma also provides some 0600 and 1800 UTC soundings]. The data provided in GIO are only those that have been assimilated (input data rejected or thinned during assimilation are not included). In the central U.S. region, the radiosonde observations tend to be grouped in the southern third, with another group of stations near the northern third. Over time, the spatial distribution of the stations does not noticeably change (not shown). Of course, when looking at the vertical distribution, mandatory levels have substantially more observations than significant levels. The temporal variability of the radiosonde data contains many changes: some large, some more subtle. It is difficult to account for every

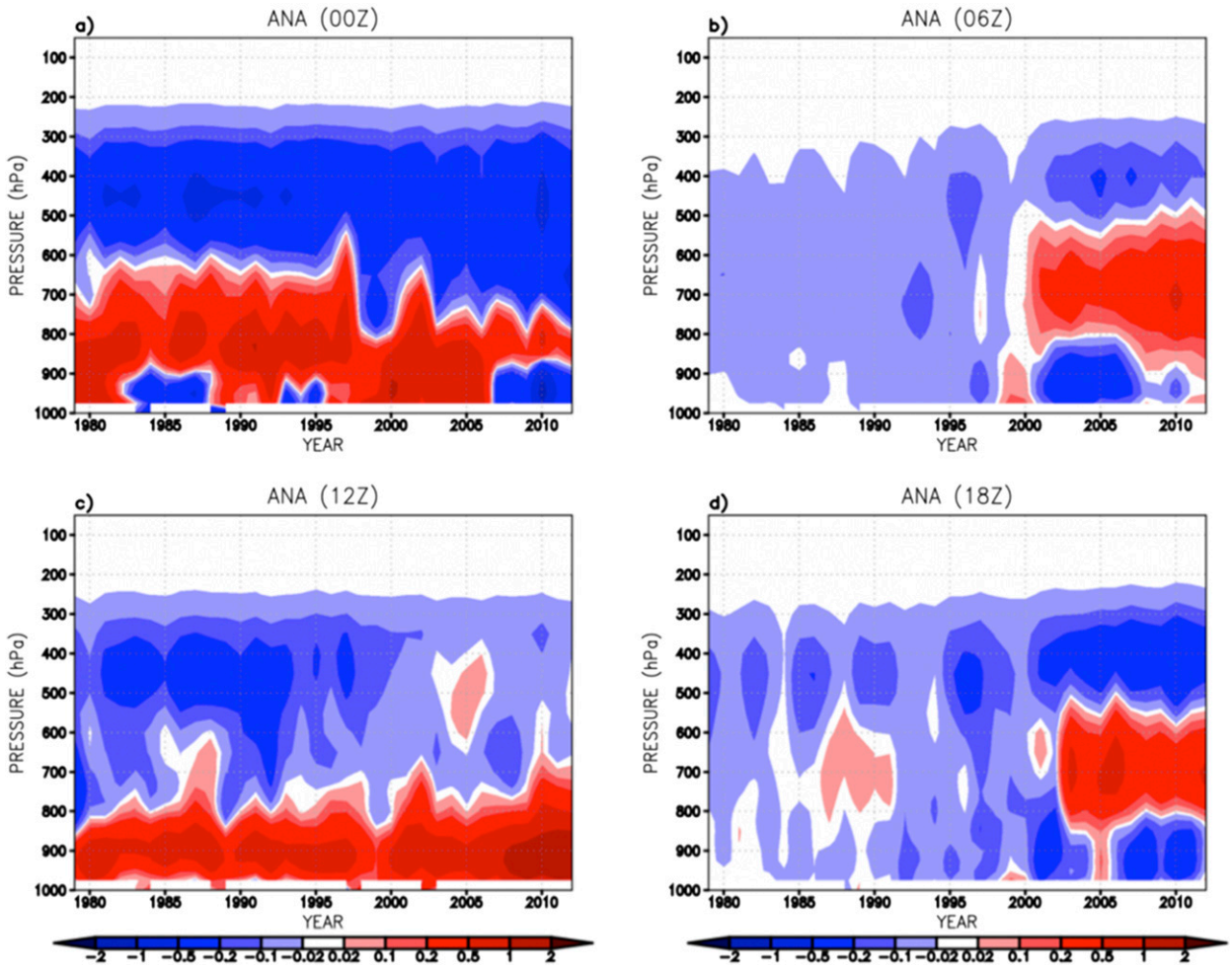

FIG. 9. Time–height cross section of annual-mean water analysis increment (g kg^{-1} day^{-1}) at (a) 0000, (b) 0600, c) 1200, and d) 1800 UTC over the central United States.

fluctuation in the time series, though the introduction of 925 hPa as a mandatory level appears around 1992. There are numerous changes in radiosonde instrumentation that may affect the climate record (e.g., Elliott et al. 2002). In MERRA, certain shifts and biases have been corrected (Haimberger 2007; Rienecker et al. 2011), though these are for temperature measurements.

The observed water vapor profiles show some year-to-year variability, but there is no indication of a change in the water vapor (Figs. 12a,b) that might be related to shift in the water budget after 2000 (Fig. 4). The analysis of RAOB water vapor differs between 0000 and 1200 UTC, where the 1200 UTC forecast is steadily dry in the lower troposphere throughout the period, while the 0000 UTC forecast shows fluctuations especially nearer the surface (Figs. 12c,d). There is a distinct separation of positive and negative forecast bias between the upper and lower troposphere. The level of this separation seems to decrease in altitude for 0000 UTC and increase for 1200 UTC after 2000 (this can also be identified in the budget's analysis increment; Figs. 9a,c). It is clear that these variations are not consistent with the sudden change in the total increment at 0600 and 1800 UTC (Figs. 9 and 10). The radiosondes provide some stability (regarding analyzed data) for the 1200 and 0000 UTC analysis. However, it is of note that the RMS of the radiosonde forecast departures decrease over the reanalysis period (primarily in the significant level observations), all the way through to the most recent years (Figs. 12e,f). The mandatory radiosonde levels also show lower RMS of the forecast departures than the significant levels.

The comparison of the ANA and MFD tendencies shows that, for this region, they are correlated well at large space and time scales (e.g., Figs. 2 and 3). While the ANA term is generally related to the water vapor analysis, MFD would be a function of both moisture and

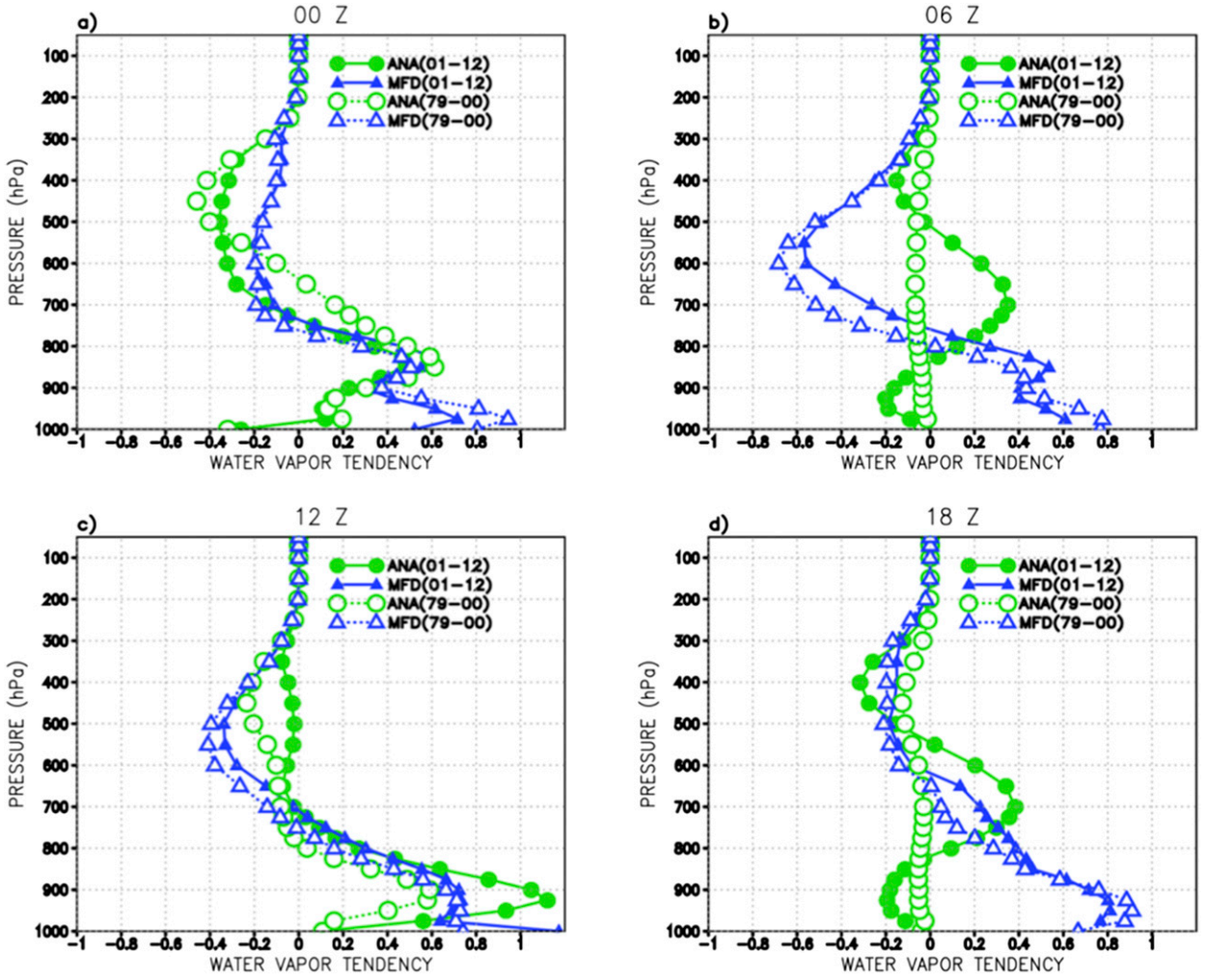

FIG. 10. Vertical profiles of water vapor tendency ANA and MFD terms at (a) 0000, (b) 0600, (c) 1200, and (d) 1800 UTC over the central United States for period 1979–2000 (dot lines) and 2001–12 (solid lines). All units are in g kg^{-1} day^{-1}.

wind. The previous discussion suggests that radiosonde water vapor assimilation is not likely involved with the shift in water vapor increments. Conventional wind observations are somewhat more complicated, considering that wind observations are available in all the analysis cycles. There tend to be some increases in the aircraft wind observations after 2000, when velocity azimuth display (VAD) wind profiles start to be assimilated. Some time was taken to evaluate the wind observing system as was presented with the radiosonde water vapor observations. While there are changes to the observing systems around 2000 because of the increase in number of observations (Fig. 13), it is not clear that these would lead to a systematic change in the moisture flux divergence. The wind increment change would need to be arranged as to increase divergence. Such a persistent arrangement seems unlikely to occur and maintain and was not obvious in evaluation of the background forecast and analysis winds and their computation of divergence. However, wind observations do serve to demonstrate the complexities of the observing system and also the difficulty in determining the physical response of the system to analyzed observations.

b. *Satellite observation sensitivity*

As diverse as the conventional observations are (including satellite data retrievals of physical quantities), the satellite radiances that are assimilated add complexity and data volume to the input data records. In this first version of GIO, we have elected to simplify the satellite data by not producing grids every 6 h, as with conventional data, but provide monthly and monthly diurnal cycle (four analysis times per month). These include the average brightness temperatures and

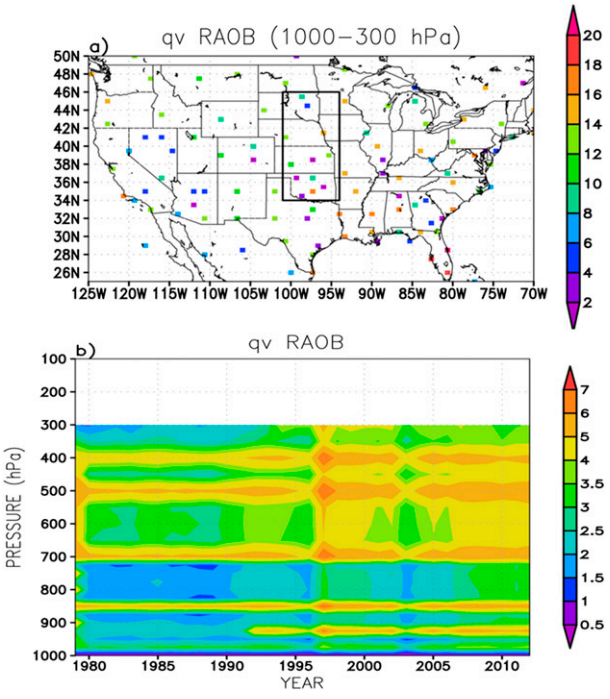

FIG. 11. Annual-mean number of water vapor (qv) observations (in thousands) for (a) RAOB stations in the United States from 1000 to 300 hPa (21 constant pressure levels) and (b) time–height cross section over the central U.S. box.

forecast departures for each month including the data count for each grid point. Consider that each instrument has multiple channels and spatial distribution at each analysis time. Multiple instruments may exist at any given time and any given region, though whether their orbits allow for observations to coexist and be assimilated in a given analysis cycle is not necessarily easily diagnosed. We first look at the available satellite observations in the region of interest to ascertain any obvious changes in the satellite observing system that may lead to changes in the analysis increment and water budget.

Rienecker et al. (2011) present a table of satellite systems assimilated in MERRA. Notably, *NOAA-15*'s introduction of the AMSU-A instrument in late 1998 led to significant shift in the global water cycle, though it appeared most influential over certain oceanic regions and land-region water cycle variations did not stand out (Robertson et al. 2011; Bosilovich et al. 2011). However, as discussed previously, the changepoint detection applied to the central United States shows spikes for 0600 and 1800 UTC at April 2001, not long after the introduction of the first AMSU-A (September 1998).

As an example, Fig. 14 shows the data count for AMSU-A channel 2 (a window channel) assimilated in MERRA for the central U.S. region. When *NOAA-15* AMSU-A is introduced (a.m. orbit), only a very small number of observations occur in the central United States at 1800 UTC and none in the 0600 UTC analysis. However when *NOAA-16*'s p.m. orbit is introduced (November 2000), coverage is primarily in 0600 and 1800 UTC in the central United States (crossing time drift affects the *NOAA-16* data counts over time). The assimilated AMSU-A channel 2 data count also has a seasonal cycle peaking in the warm season (all window channels exhibit a similar seasonality, not shown). So, any seasonally varying *NOAA-16* data (e.g., AMSU-A, AMSU-B, and HIRS3) assimilation first appears in 0600 UTC analysis in the 2001 warm season. *Aqua* AMSU-A is assimilated beginning in the end of 2002, so that 2003 is the first warm season where that instrument is used. Its 0600 and 1800 UTC counts indicate it is also of significance for water vapor in the seasonal cycle.

By the end of 2007, both *NOAA-16* and *Aqua* AMSU-A channel 4 experience problems and are turned off (all of *NOAA-16* AMSU-A is not assimilated after then). However, the *Aqua* AMSU-A window and other channels continue to be assimilated after channel 4 is excluded. Starting in 2008, the number of *Aqua* AMSU-A window channel observations being assimilated increases in the central U.S. region. In addition, *NOAA-17* only provided data for a limited period of 2005–06, while *NOAA-18* started providing data in 2006. Considering the data counts suggests that the *NOAA-16* overpass of the central U.S. region could affect the 0600 and 1800 UTC analyses, while *Aqua* in 2003 appears concurrent with significant variations in the 1800 UTC analysis (cf. Figs. 14 and 9). It is also worthwhile to note that the 1800 UTC analysis window includes the local solar noon time and associated surface heating.

Figure 15 shows the forecast departures (OmF) at each analysis cycle for each platform's AMSU-A channel 5 radiance (a channel sensitive to lower troposphere temperature). At 0600 UTC, the forecast departures are positive, although, each analysis cycle seems to have its own temporal variations. The *NOAA-15* AMSU-A channel 5 forecast departures exhibit a gradual trend at 0000 UTC, but at 1200 UTC they jump near 2008, along with the other available AMSU-A instruments. Channel 5 data counts (not shown) generally follow the relative pattern of channel 2 data counts (Fig. 14). It is worthwhile noting that the *NOAA-15* and *NOAA-18* channel 4 forecast departures and analysis increments rise sharply following the loss of *NOAA-16* AMSU-A and *Aqua* AMSU-A channel 4 (not shown). AMSU-A channel 4 is sensitive to the water burden in the lower troposphere, and the change in available data affects the analysis of other channels.

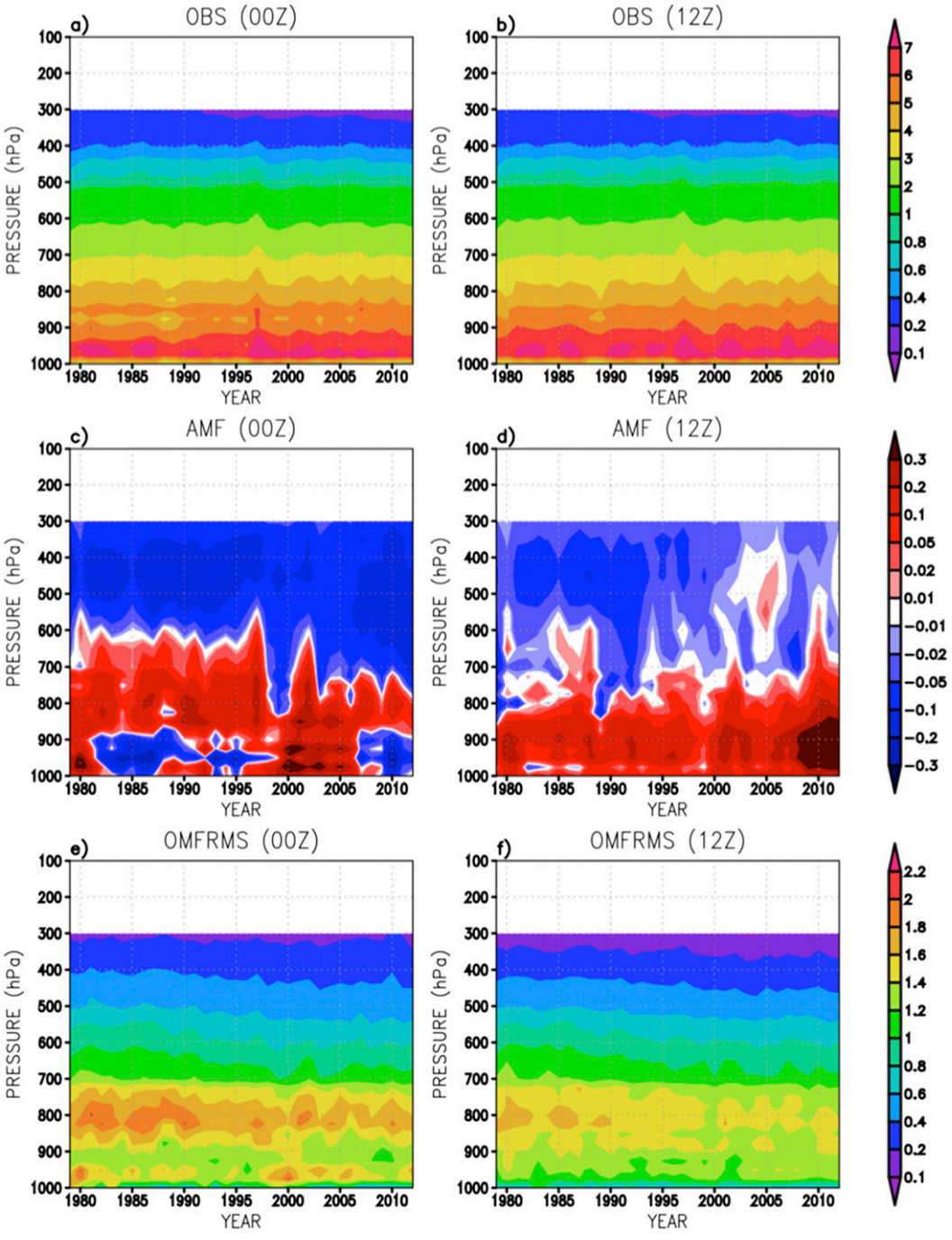

FIG. 12. (top) Annual-mean water vapor mixing ratio observations, (middle) analysis increment at the observation locations, and (bottom) root-mean-square error of forecast departure from RAOB water vapor over the central United States at (left) 0000 and (right) 1200 UTC. All units are in grams per kilogram.

As MERRA production evolved with longer time series, it was not immediately obvious that AMSU-A should be as influential on the U.S. regional water cycle, as this evaluation shows. Early sensitivity tests showed strong signals over the southern oceans and warm pool regions than over land (e.g., Bosilovich et al. 2011). However, we now see the impact of observing system variations, especially from remote sensing platforms over land, was obscured by the variations in the diurnal cycle and the presence of radiosonde observations. Even so, aboard the NOAA satellites are also HIRS3 and AMSU-B instruments, each with

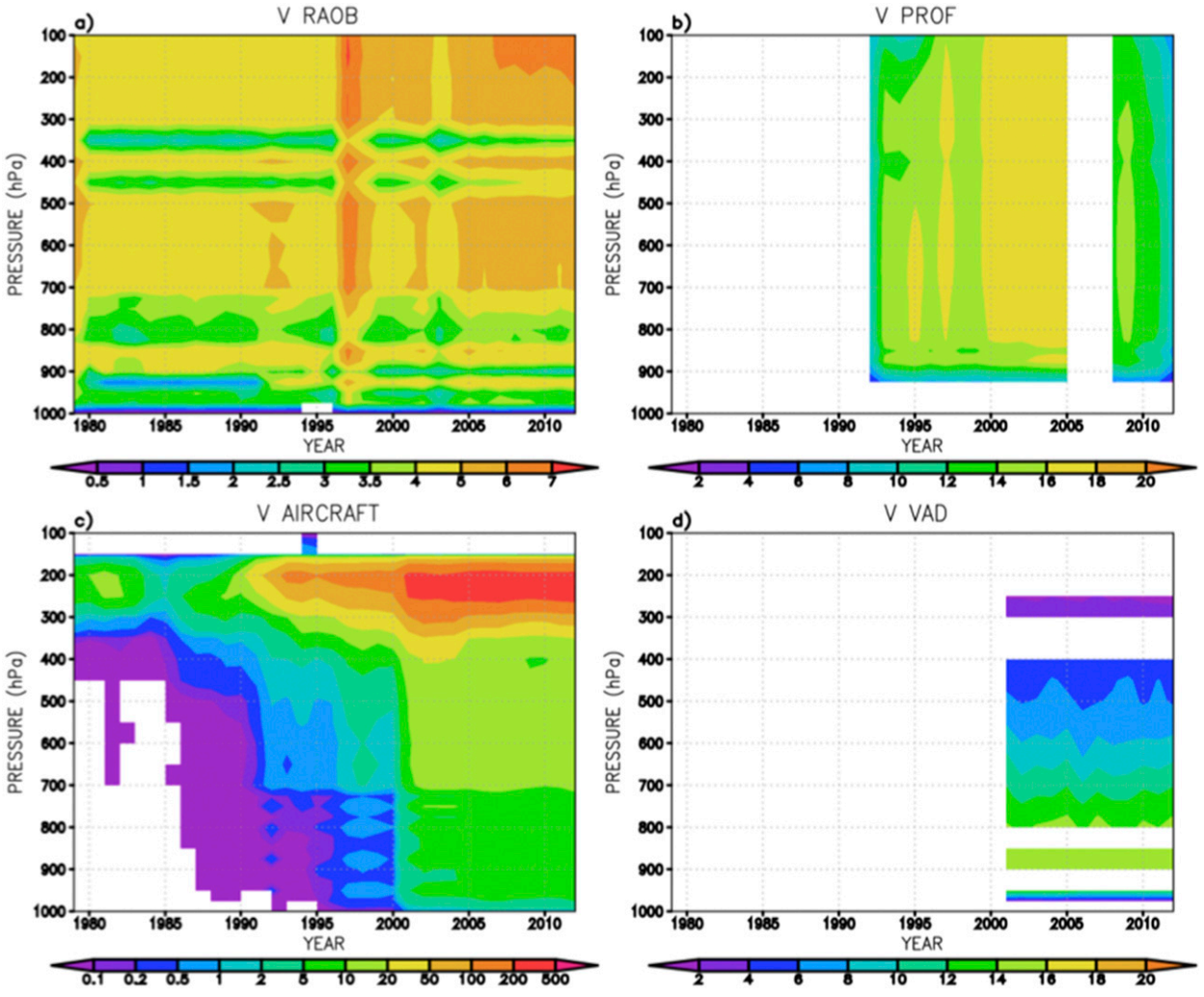

FIG. 13. The annual number of meridional wind observations (in thousands) over the central United States for wind from (a) radiosonde, (b) wind profiler network, (c) aircraft, and (d) VAD. A technical coding error lead for the MERRA input data lead to the wind profiler gap during 2006–07.

channels sensitive to the water vapor [though their impact on global and hemispheric forecast error tends to be less than AMSU-A, as discussed by Gelaro and Zhu (2009)]. Likewise, AMSU-B and HIRS3 instruments occasionally have different availability in the historical record because of instrument or channel failures. Atmospheric Infrared Sounder (AIRS) is another consideration, with more than 150 channels assimilated in MERRA, it holds the largest volume of data used in MERRA, though the impact of AIRS on global forecast error is also less than AMSU-A (Gelaro and Zhu 2009).

To define which instrument(s) contributes to the water vapor analysis increment profile that causes the MFD signal in the central United States, we performed a series of data withholding experiments, individually removing AMSU-B, HIRS3, AMSU-A, and AIRS. Since the signal in the analysis increments peaks in summer and also occurs with regularity between 2001 and 2006, we performed the sensitivity tests for one month, July 2005, on each instrument. Figure 16 shows the control analysis increment for July 2005 and the contribution of each instrument to that increment, as determined by individually withholding that instrument. The impact on the anomalous water vapor increments in the central United States is not related to HIRS3 or AMSU-B assimilation. The small effect of these channels may be in line with the assimilation of previous instruments, like HIRS2, considering the 0600 and 1800 UTC increments early in the reanalysis period shown in Fig. 9.

Withholding AMSU-A largely removed the 0600 UTC drying increments below 850 hPa and a fraction of increments above 700 hPa. The assimilation of AIRS accounts for the strong positive water vapor increments

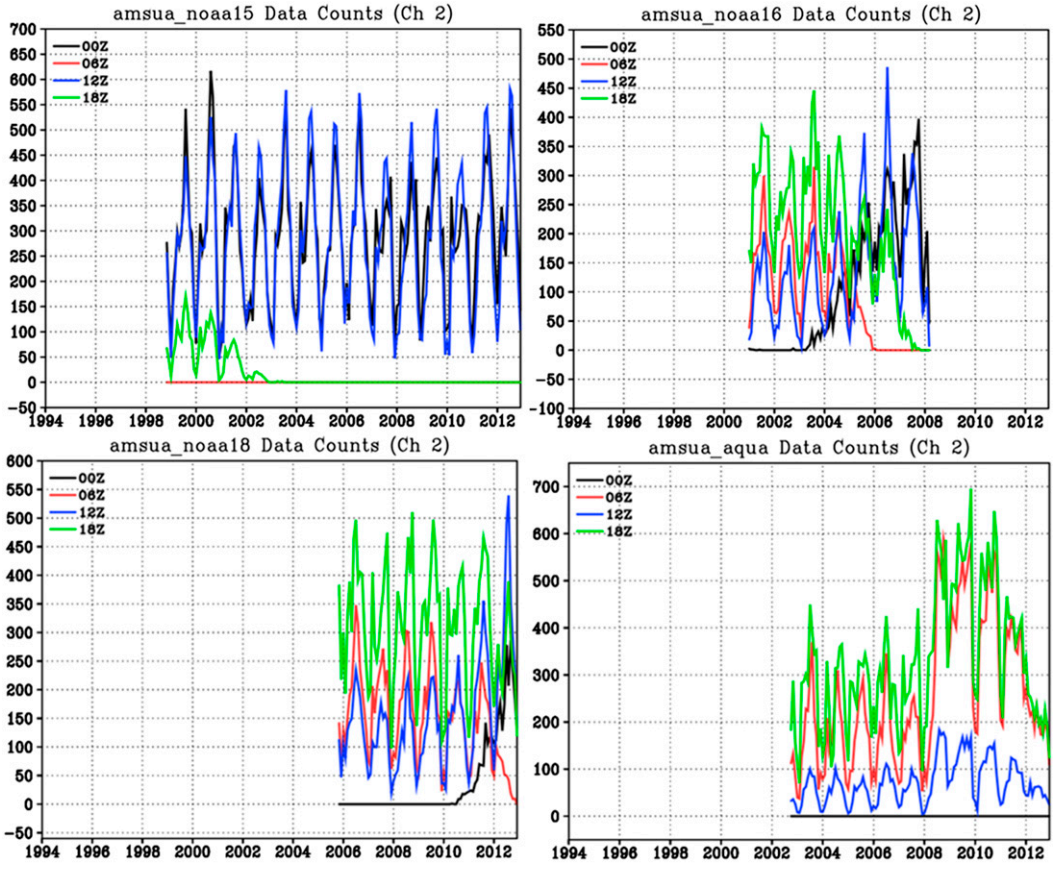

FIG. 14. Monthly data count over the central U.S. region for all platforms: (a) *NOAA-15*, (b) *NOAA-16*, (c) *NOAA-18*, and (d) *Aqua*, of AMSU-A window channel 2, where each line indicates an analysis time. Lines may overlap, especially if no observations were present. These counts reflect the observations that were assimilated and not the actual number of observations that may be available. Also, data thinning affects the number reported here.

centered at 700 hPa in the 0600 UTC analysis. In the 1800 UTC analysis, AMSU-A is causing the large positive increments at 700 hPa with some contribution from AIRS, though the AIRS contribution to drying above 500 hPa is also apparent. Subsequent tests were designed to identify the AMSU-A channels, leading to the strong water vapor increments. AMSU-A window channels (1, 2, 3, and 15) are the primary cause of the boundary layer drying increments (Fig. 17). In the 1800 UTC analysis, the window channels are only partly contributing to the peak source of water at 700 hPa. The other part (from 700 hPa to the surface) comes from channel 5, which is sensitive to the atmospheric temperature. Channel 4, which is sensitive to the water vapor, plays a much smaller role on the water vapor increments but does add water at 700 hPa and remove water in the PBL. It is also worthwhile to mention that ERA-Interim did not assimilate AMSU-A window channels, which emphasizes the result that their central U.S. anomaly is related to different reasons. In subsequent NASA reanalyses, AMSU-A window channels will not be included in the assimilation for impacts much more global than identified here (Rienecker et al. 2011). At this point, we have not tried to isolate the AIRS channel contributions. The influence and appropriateness of AIRS and AMSU-A channel 5 on the continental U.S. water vapor increments will require further study.

5. Summary and conclusions

Reanalyses continue to be developed and improved over time, and the research community demands more quality and detail in global and regional processes. However, the crucial underlying observing system is a complex collection of diverse variables, each with incomplete spatial and temporal coverage. Ideally, we would like to be able to assess inconsistencies in the resulting reanalysis and identify physical improvements to the system, such as the suggestion to incorporate irrigation as a source of water in the central United States to improve the water cycle there [as suggested by Trenberth et al. (2011) in regards to Fig. 1]. In this study, we

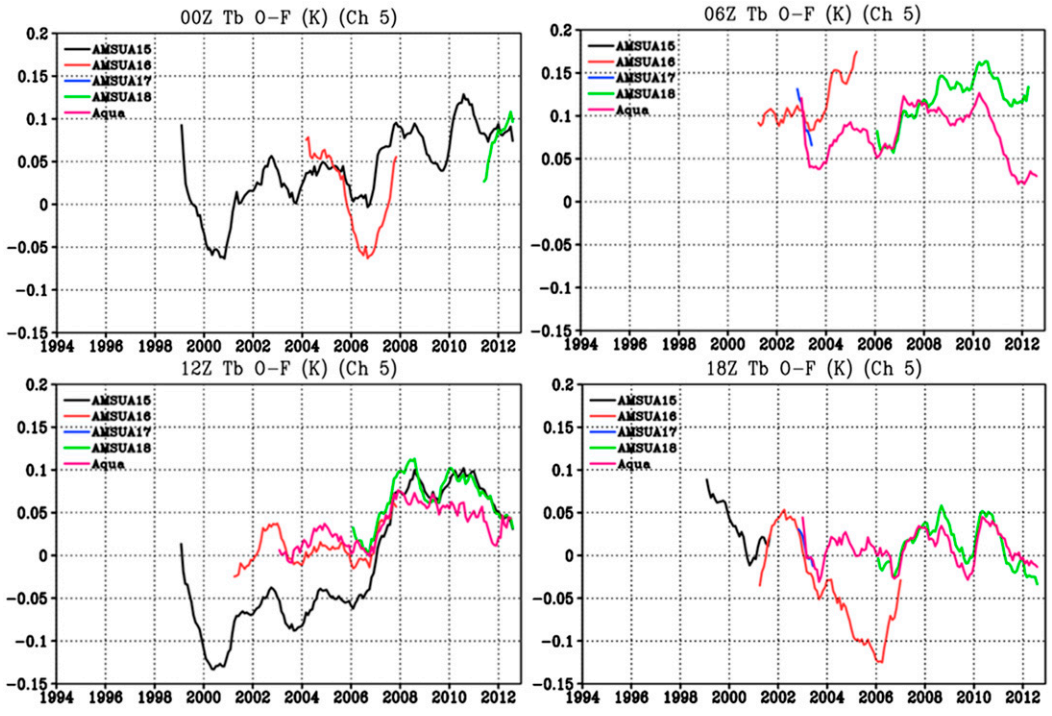

FIG. 15. Monthly forecast departures (OmF) for AMSU-A channel 5 brightness temperatures (K) over the central U.S. region, separated by analysis time.

investigate a deficiency in the physical fields of the regional water budget of the central United States and then use the closed regional water budget, three-dimensional water vapor analysis increments, and assimilated observations to evaluate the reanalysis data.

Vertically integrated water vapor increments are related to an anomalous MFD feature presented in Fig. 1, which starts in the early 2000s but before that had more realistic features (i.e., the negative divergence implies more precipitation than evaporation). The vertically integrated MFD and increments only revealed part of the problem, as there was a distinct positive increment, yet precipitation decreased while the divergence increased. This is explained by looking at the vertical profiles of MFD and the analysis increment but only after the diurnal variations of the four analysis cycles are considered individually. In particular, significant contrasts occurred when radiosonde data are more

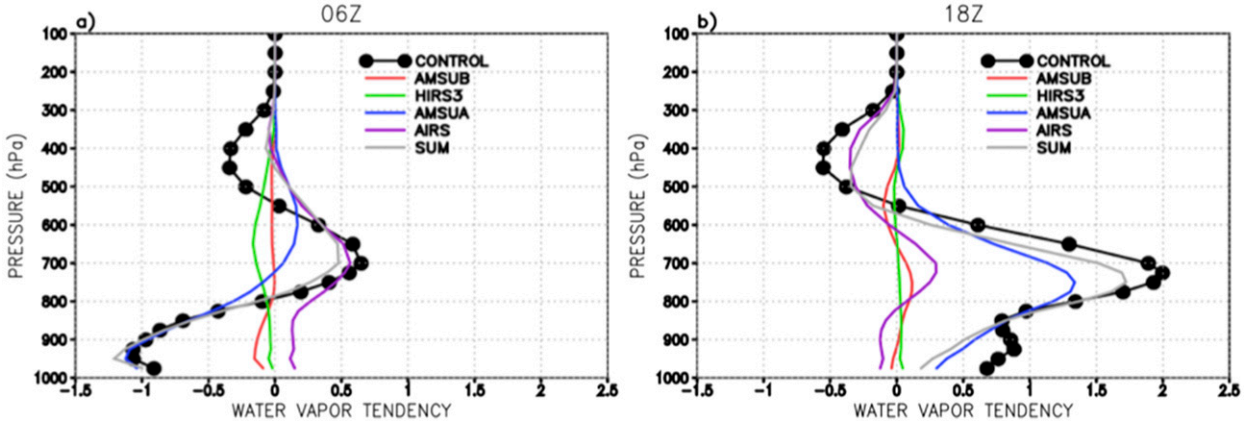

FIG. 16. Contribution of selected instruments (AMSU-A, AMSU-B, HIRS3, and AIRS) to monthly-mean ANA tendency ($g\,kg^{-1}\,day^{-1}$) at (a) 0600 and (b) 1800 UTC over the central U.S. region in July 2005. Control experiment (CONTROL) has all observations as MERRA. The contribution of each instrument is the difference between the control experiment and each instrument's data withholding experiment. "SUM" is the summation of AMSU-A, AMSU-B, HIRS3, and AIRS.

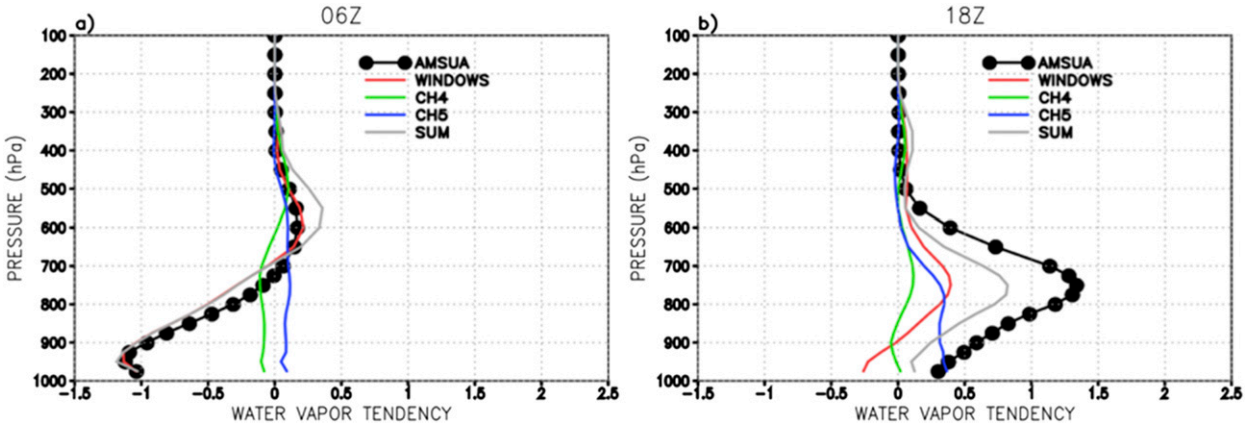

FIG. 17. Contribution of AMSU-A and its selected channels (window channels, channel 4, and channel 5) to monthly-mean ANA tendency (g kg^{-1} day^{-1}) at (a) 0600 and (b) 1800 UTC over the central U.S. region in July 2005. Window channel includes channels 1, 2, 3, and 15. The contribution of each channel is the difference between the control experiment and each channel's data withholding experiment. "SUM" is the summation of window channels, channel 4, and channel 5.

influential (0000 and 1200 UTC) than when there are few radiosonde observations (0600 and 1800 UTC). The water vapor increments change dramatically around March 2001 but especially in the 0600 and 1800 UTC analysis cycles, where water vapor is added above the boundary layer and the analysis increments were taking away water in the lowest layer. While 0000 and 1200 UTC profiles of the water budget terms change around this time, the vertical structure of the profiles, constrained by the strong presence of radiosonde profiles, is similar in the early and late periods considered. This time of change is also collocated with the first warm season to include *NOAA-16* data assimilation, including AMSU-A, AMSU-B, and HIRS3. *NOAA-16*'s orbit at launch covered the central United States during the 0600 and 1800 UTC analysis cycles initially (crossing time drift affects that over a period of years). However, the *Aqua* AMSU-A and AIRS instruments began providing data at the end of 2002 and also contributed to the 0600 and 1800 UTC analysis cycles in the central United States. Observing system experiments narrowed the source of the changing analysis increments (and hence MFD) to the assimilation of AMSU-A window channels and channel 5 but also AIRS.

The GIO data provide a fundamental part of evaluating the observing system and its variations in time over this region. The gridding permits quantitative evaluation that can be performed across all the assimilated observations, from radiosonde to radiance. While these data are produced for all reanalyses, they are generally in formats that require additional time and effort to use, and access to them may also be more challenging than the reanalysis products themselves. The gridded observations guided sensitivity tests to isolate the systems that affect the water vapor increments in the central United States. In subsequent work, we hope to evaluate the forecast departure and analysis increments of each observing type, along with more advanced diagnostics of the analysis (e.g., Desroziers et al. 2005). Likewise, we are revisiting the formulation of the gridding process to provide as much information about the analysis. For example, this initial form of GIO did not include the variational bias corrections used for radiance assimilation (Dee and Uppala 2009), and that could provide additional information to evaluate the various observing systems and channels.

Acknowledgments. This work was supported by NASA's Energy and Water Cycle Studies program (NEWS) and also the NASA's Modeling and Analysis Program (MAP). Adrian Simmons and two anonymous reviewers provided thorough and constructive reviews that greatly helped the final form of the manuscript. Several discussions with Ron Gelaro, Will McCarty, Ricardo Todling, and Meta Sienkiewicz on the observing system and data assimilation were vital in development of this work. King-Sheng Tai's effort in producing the sensitivity studies is greatly appreciated. We also thank Christopher Redder for his initial efforts in developing the GIO data files.

APPENDIX

Acronyms

AIRS	Atmospheric Infrared Sounder
AM	Here, referring to a satellite's morning sun-synchronous orbit
AmF	Analysis minus forecast
AMSU	Advanced Microwave Sounding Unit (sometimes with versions A and B)

ANA	Indicates the analysis increment term of the reanalysis water vapor budget
ARM SGP	U.S. Department of Energy's Atmospheric Radiation Measurement Southern Great Plains facility
ATOVS	Advanced TIROS Operational Vertical Sounder
CMAP	Climate Prediction Center (CPC) Merged Analysis of Precipitation
CPCU	Climate Prediction Center (CPC) Unified Precipitation Analysis
ECMWF	European Centre for Medium-Range Weather Forecasts
ERA-Interim	Interim ECWMF Re-Analysis
GEOS5	Goddard Earth Observing System, version 5
GIO	Gridded Innovations and Observations
GMAO	Global Modeling and Assimilation Office
GPCP	Global Precipitation Climatology Project
HIRS	High-resolution Infrared Radiation Sounder
IAU	Incremental analysis update
MERRA	Modern Era Retrospective-Analysis for Research and Applications
MFD	Moisture flux divergence
MSU	Microwave Sounding Unit
NASA	National Aeronautics and Space Administration
NOAA	National Oceanic and Atmospheric Administration
OmA	Observations minus analysis
OmF	Observation minus forecast
PBL	Planetary boundary layer
PM	Here, referring to a satellite's sun-synchronous afternoon orbit
RAOB	Radiosonde observation
SSM/I	Special Sensor Microwave Imager
SSU	Stratospheric sounding unit
TIROS	Television Infrared Observation Satellite

REFERENCES

Bloom, S., L. Takacs, A. da Silva, and D. Ledvina, 1996: Data assimilation using incremental analysis updates. *Mon. Wea. Rev.,* **124,** 1256–1271, doi:10.1175/1520-0493(1996)124<1256:DAUIAU>2.0.CO;2.

Bosilovich, M. G., F. R. Robertson, and J. Chen, 2011: Global energy and water budgets in MERRA. *J. Climate,* **24,** 5721–5739, doi:10.1175/2011JCLI4175.1.

Dee, D. P., and S. Uppala, 2009: Variational bias correction of satellite radiance data in the ERA-Interim reanalysis. *Quart. J. Roy. Meteor. Soc.,* **135,** 1830–1841, doi:10.1002/qj.493.

——, and Coauthors, 2011: The ERA-Interim reanalysis: Configuration and performance of the data assimilation system. *Quart. J. Roy. Meteor. Soc.,* **137,** 553–597, doi:10.1002/qj.828.

Desroziers, G., L. Berre, B. Chapnik, and P. Poli, 2005: Diagnosis of observation, background and analysis-error statistics in observation space. *Quart. J. Roy. Meteor. Soc.,* **131,** 3385–3396, doi:10.1256/qj.05.108.

Elliott, W. P., R. J. Ross, and W. H. Blackmore, 2002: Recent changes in NWS upper-air observations with emphasis on changes from VIZ to Vaisala radiosondes. *Bull. Amer. Meteor. Soc.,* **83,** 1003–1017, doi:10.1175/1520-0477(2002)083<1003:RCINUA>2.3.CO;2.

Gelaro, R., and Y. Zhu, 2009: Examination of observation impacts derived from observing system experiments (OSEs) and adjoint models. *Tellus,* **61A,** 179–193, doi:10.1111/j.1600-0870.2008.00388.x.

Haimberger, L., 2007: Homogenization of radiosonde temperature time series using innovation statistics. *J. Climate,* **20,** 1377–1403, doi:10.1175/JCLI4050.1.

Kanamaru, H., and G. D. Salvucci, 2003: Adjustments for wind sampling errors in an estimate of the atmospheric water budget of the Mississippi River basin. *J. Hydrometeor.,* **4,** 518–529, doi:10.1175/1525-7541(2003)004<0518:AFWSEI>2.0.CO;2.

Lund, R., and J. Reeves, 2002: Detection of undocumented change points: A revision of the two-phase regression model. *J. Climate,* **15,** 2547–2554, doi:10.1175/1520-0442(2002)015<2547:DOUCAR>2.0.CO;2.

Ozdogan, M., and G. Gutman, 2008: A new methodology to map irrigated areas using multi-temporal MODIS and ancillary data: An application example in the continental US. *Remote Sens. Environ.,* **112,** 3520–3537, doi:10.1016/j.rse.2008.04.010.

——, M. Rodell, H. Kato Beaudoing, and D. L. Toll, 2010: Simulating the effects of irrigation over the United States in a land surface model based on satellite-derived agricultural data. *J. Hydrometeor.,* **11,** 171–184, doi:10.1175/2009JHM1116.1.

Reichle, R., R. D. Koster, G. J. M. De Lannoy, B. A. Forman, Q. Liu, S. P. P. Mahanama, and A. Toure, 2011: Assessment and enhancement of MERRA land surface hydrology estimates. *J. Climate,* **24,** 6322–6338, doi:10.1175/JCLI-D-10-05033.1.

Rienecker, M. R., and Coauthors, 2011: MERRA: NASA's Modern-Era Retrospective Analysis for Research and Applications. *J. Climate,* **24,** 3624–3648, doi:10.1175/JCLI-D-11-00015.1.

Roads, J. O., M. Kanamitsu, and R. Stewart, 2002: CSE water and energy budgets in the NCEP–DOE Reanalysis II. *J. Hydrometeor.,* **3,** 227–248, doi:10.1175/1525-7541(2002)003<0227:CWAEBI>2.0.CO;2.

Robertson, F. R., M. G. Bosilovich, J. Chen, and T. L. Miller, 2011: The effect of satellite observing system changes on MERRA water and energy fluxes. *J. Climate,* **24,** 5197–5217, doi:10.1175/2011JCLI4227.1.

Trenberth, K. E., J. T. Fasullo, and J. Mackaro, 2011: Atmospheric moisture transports from ocean to land and global energy flows in reanalyses. *J. Climate,* **24,** 4907–4924, doi:10.1175/2011JCLI4171.1.

Uppala, S. M., and Coauthors, 2005: The ERA-40 Re-Analysis. *Quart. J. Roy. Meteor. Soc.,* **131,** 2961–3012, doi:10.1256/qj.04.176.

Yarosh, E. S., C. F. Ropelewski, and E. H. Berbery, 1999: Biases of the observed atmospheric water budgets over the central United States. *J. Geophys. Res.,* **104,** 19 349–19 360, doi:10.1029/1999JD900322.

Yokoi, S., 2015: Multireanalysis comparison of variability in column water vapor and its analysis increment associated with the Madden–Julian oscillation. *J. Climate,* **28,** 793–808, doi:10.1175/JCLI-D-14-00465.1.